Investigative Analysis on Residual Stresses Generated In Castings

Poralla Naveen Kumar Reddy[1], N.Phani Raja Rao[2]
[2] Assistant Professor
[1, 2] SVIT Engineering College, Hampapuram, Anantapur

Abstract- *Unpredictable residual stresses are in most components considered to be a defect. The stresses are formed during the cooling process, caused by the temperature and visco plastic strains. Performing a heat treatment (HT), the material starts to creep and residual stresses can be reduced with over 90% of the total initial stress. This study has been done in order to examine residual stress relieving in the HT for three cast iron materials, VIG-275/190, GJL-250 and GJS-500-7. The purpose is to find the effect of varying parameters and compare the result against simulation. A stress lattice component, designed to create residual stress are used to investigate the stress relieving. Through a sectioning method the stress is released and can be measured by strain gauges placed on the surface. The stresses are measured on each material both as cast and after HT and trough empirical testing the effect of different parameters during the HT was established. Comparing the practical test against simulations by Magma5 the cooling rate during solidification process is too quick in simulations. This fault is attributed to the non-included latent heat release during phase transformation at 723 °C (austenite to pearlite). By changing the specific heat capacity of sand and the cast iron this error can be corrected. The simulations also predict the stress to be fully relieved when reaching the hold temperature of 610 °C, this have been confirmed to be wrong shown by the significant effect of hold time in all investigated materials. The effects of varying cooling rates and drop temperatures are also difficult for the simulations to predict. Heat treatment experiments on of VIG-275/190 shows that the alloying of Molybdenum and Chromium makes the material more resistant against creep at elevated temperatures. The hold time and time spent over 500 °C are the most significant parameters. The unalloyed GJL-250 creeps more easily which makes all the heat treatment parameters more important, i.e. heating rate, hold time and cooling rates. Lastly the ductile iron GJS-500-7 has the highest residual stress in as cast condition and shows the largest stress relief after the heat treatments.*

Keywords- Heat Treatment, X-Direction, Solidification, GJL, GJS

I. INTRODUCTION

When the melted metal in a casting process cools down and solidifies, residual stresses arise from the strain caused by viscoplastic flow and temperature gradients. This is because the thermal energy dissipates faster in the thinner sections compared to the thicker sections and causes a temperature gradient in the material leading to residual stresses. While the thinner part is contracting due to the thermal contraction the core is still hot and maintains its larger volume. When the material is further cooled to room temperature the differences in thermal contractions cause residual stresses. In order to get rid of these stresses heat treatment is required. Residual stresses have a significant effect on the materials mechanical properties and the overall performance. High residual stresses can lead to early fatigue, increased crack propagation and potentially fracture the component.

After the solidification process, cast iron components are heat treated to reduce the residual stresses. This will improve the mechanical properties and avoid undesired stress concentrations in the material. As an example a cylinder head has a complex geometry and residual stresses are unwanted and difficult to predict. The assumption is that these stresses can be counteracted and lowered to insignificant levels with a heat treatment. By investigating varying heat treatment parameters and relate them to the relieving of residual stresses a process optimization can be done. This could in turn lead to higher quality components and improve the overall manufacturing process.

The materials that will be investigated are shown below, specific material properties are shown in chapter Investigated materials.

Grey iron, GJL-250
Grey iron, VIG 275/190 Ductile iron EN-GJS-500-7

SOLIDIFICATION

The software Magma5 simulates solidification and heat treatment to predict the residual stresses. Simulations

save both time and money but have requirements on accuracy and precision to be reliable. Finding discrepancies between practical tests and simulations would bring new aspects to improve the simulations and make them more efficient and precise.

The phenomena of melting and solidification has many current engineering applications such as ice formation, solidification of castings and scrap melting in the metal industry, the cooling, freezing and cold storage of foodstuffs in the food industry and certain other problems in chemical engineering (Mastanaiah, 1976).

Among them casting industry is one of the oldest industries in human society and until recently, it was considered to be an art rather than a science. Only after the Second World War, the basic variables in the process of casting industry have been studied in details to have a greater understanding of the interrelations of the factors involved in making a good casting. The foundry technology is fast becoming an applied science with much of mathematical formulae. But still the subject is not yet a complete science because of the number of variable factors involved. With the help of computers, now we are in a better position to tackle metal casting from a scientific point of view.

There are number of casting processes available depending upon the nature of the product. It involves considerable metallurgical and mechanical aspects. Properly designed dies and a good control over the process parameters are considered a must for quality castings. To arrive at the optimum process parameters, the experimental methods are always better than simulations. But from realistic considerations, it is costly and time consuming and many are impossible in some cases. Hence computer simulation of the whole process is a convenient way to design a mould and analyze the effects of various parameters.

METAL CASTING

It is a phase transformation process of liquid to solid state. A metal in molten condition possesses high energy. As the melt cools, it looses energy to form crystals. The crystal growth proceeds with release of energy at the crystal melt interface. Solidification process exerts a very strong influence upon the three properties of cast metal viz.

(i) Segregation of alloying elements,
(ii) Microstructure (i.e.) grain size and phases present
(iii) Soundness (i.e.) porosity in the metal.

During solidification, cast form develops cohesion and acquires structural characteristics. Also during solidification, casting acquires the metallographic structures viz. grain size, shape and its orientation, distribution of alloying elements and under lying crystal structures and its imperfections.

The rate of cooling governs the microstructure of casting to a large extent and intern it controls mechanical properties like strength, hardness, machinanability, etc. The magnitude of residual stresses built-up in the casting depends on the geometry of the casting, mould design and thermo mechanical properties of both the cast and the mould process parameters.

In case of very high residual stress accumulation, the casting may develop cracks at the time of processing itself. Low residual stresses may not be high enough to cause cracks during processing but sufficiently high enough to reduce the fatigue life leading to early failure in service.

FACTORS OF SOLIDIFICATION

Many phenomena contribute to the overall casting process, including heat transfer, fluid flow, thermal stress, solidification kinetics, species flow analysis, etc. Since the thermal history of a casting is the driving force, the other phenomena, an understanding of the thermal history can be used to predict stresses, microstructure and defects.

Pure metals melt and solidify at the same temperature under equilibrium conditions. The metal is completely solid below that temperature. Whereas alloys solidify over a range of temperature. Above that range the metal is in liquid phase, below that range, it is in solid phase and during that range it is in both liquid and solid phase, called as mushy. The major features of the solidification phenomena include transient process, latent heat liberation and air-gap formation between the casting and the mould.

II. EXPERIMENTAL WORK & MATERIALS

This chapter describes the theory behind the experimental analysis as well as the collection of useful information to evaluate the results. Each step of both the practical and simulation experiments is done on all investigated materials, with the exception of simulation of GJL-250.

III. MEASURE RESIDUAL STRESSES WITH SECTIONING METHOD

The elongation (length difference in %) is measured using a strain gauge. Using only one gauge is not sufficient; several gauges are required in order to accumulate accurate data. The strain gauge is a simple technological tool and yet precise and accurate when measuring resistance.

To measure elongation the strain gauge is fixated into the test pieces surface with a suitable adhesive. The adhesive must cover all of the thin copper wiring to ensure that errors are kept small. The setup of the gauge is simple and uses a Wheatstone bridge to calculate the resistance in the strain gauge. The Wheatstone bridge is the electrical circuit shown in Fig. Rgauge has an unknown resistivity and can be calculated by knowing all the other resistances. The unknown resistivity changes depending on strain of the section and can thus be used as a way to measure the strain. Below Fig. describes the Wheatstone bridge and shows how the gauge is included.

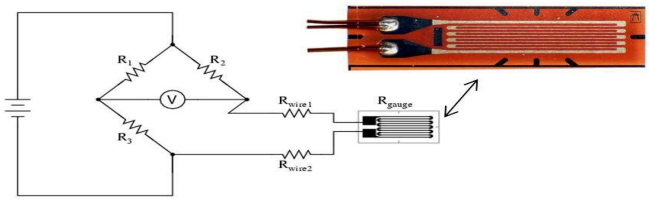

Fig. The Wheatstone bridge to measure resistance in a strain gauge

The Rgauge is what is known as the foil in the strain gauge and does a zigzag thread resemble a spring. This is to ensure that the elongation is completely elastic and makes sure that only linear elongation occurs, a necessity for precise results. The resistance is very sensitive to changes. Under tension the area of the thread becomes smaller and resistance increases. Under compressive stress the area grows larger and resistance is lowered. From this the load case and stresses can easily be determined using the equations below. From equations Eq.1 and Eq.1 below, GF is Gauge Factor, ΔR is the change of resistance, Rg is resistance before deforming and BV is the bridge excitation voltage.

Equation 1 and equation 2. The *relation used to calculate strain from measured resistance*

$$GF = \frac{\Delta R/R_G}{\varepsilon}$$

Equation 1

$$v = \frac{BV \cdot GF \cdot \varepsilon}{2}$$

Equation 2

The material used for the strain gauge is specific due to the thermal expansion that occurs during testing. The alloys have been designed so that the thermal expansion of the material cancels out by the resistance decrease due to the extra heating. Fig shows the tool used to measure the resistivity from the strain gauge. First the strain is calibrated before the sectioning is performed and will generate the first strain value ε1. After sectioning a new strain is measured ε2 and the difference is calculated as ε1-ε2. The Δε is used in Hooke's law and with a Young's modulus of 130 GPa in compressive and 120 GPa in tensile will give the stress through the lattice.

Fig. The tool used to measure the strain generated from the Wheatstone bridge to measure resistance in a strain gauge. Following is an example of how the stress is calculated from measurements:

First measure the strain ε1 from calibration of the Wheatstone bridge, e.g. 49750. After sectioning, the strain has to be measured once again; ε2 is given, e.g. 50000. This gives the total strain of sectioning (ε1-ε2 = -250), by apply the Hooke's law in compression stress (E=130 GPa) the resulting stress is E*ε= 130 GPa × -250 = -32,5 MPa.

THERMOCOUPLE

Thermocouples will be used to measure the temperature of the stress lattices in the practical experiments. The principle behind it is simple and it can measure temperature accurately enough to fulfill the demands of the testing. By joining two rods of different alloys with one another through soldering at one end and let the two pieces experience a heat change, a difference in voltage will be generated at the soldered point. The voltage generated from this type of action is called the Seebeck effect. This effect is measured in emk (electro-motive force, in this case it is referred to termo-emk because the difference in voltage is generated due to the temperature difference) and is the sum of change of potential in a circuit. On the opposite side of the

rods, the non-soldered part is then attached to a device measuring the change of voltage over the two metals and display the temperature.

INVESTIGATED MATERIALS

The experimental part will be performed and compared between three materials; Grey iron GJL-250, Grey iron VIG-275/190 and Ductile iron EN-GJS-500-7. It should be noted that the chemical composition is just for reference. Each foundry adjusts their cast iron composition to achieve the mechanical properties demanded of the iron.

Two foundries produced the stress lattices used for the experimental part, Skövde foundry and SKF's foundry.

Grey iron, VIG 275/190
Grey iron, GJL-250
Ductile Iron En-GJS-500-7

THE PRACTICAL HEAT TREATMENTS

The heat treatments that are performed have the purpose to provide information regarding how each individual parameter affects the residual stresses. Four varying parameters (heating rate, hold time, cooling rate and drop temperature) and one extra attempt at an intermediate holding time requires at least six heat treatments.

Table. The heat treatment cycles of the first seven heat treatments for VIG- 275/190:

Trial	Heating rate	Hold time	Cooling rate	Drop temperat
1	67	2,5	75	200
2	**200**	2,5	75	200
3	200	**0**	75	200
4	200	**5**	75	200
5	200	2,5	**150**	200
6	200	2,5	75	**420**

Table. The four reamining heat treatments of VIG 275/190:

Trial	Heating rate	Hold time	Cooling rate	Drop temperat
7	250	0	150	200
8	200	2,5	75	200
9	67	2,5	150	300
10	67	5	75	100

Table. The remaining heat treatments of GJL-250

Trial	Heating rate [°C/h]	Hold time [h]	Cooling rate [°C/h]	Drop temperatu re [°C]
7	200	**1h 15min**	75	200
8	200	2,5	-	600
9	200	2,5	**350**	200

Table. The reduced heat treatment plan for Ductile Iron GJS 500-7:

Attempt	Heating rate [°C/h]	Hold time [h]	Cooling rate [°C/h]	Drop temperat ure [°C]
2	200	2,5	75	200
3	200	0	75	200
4	200	**5**	75	200
5	200	2,5	**150**	200
6	200	2,5	75	**420**
7	200	2,5 @ 540 °C	75	200

IV. RESULT AND DISCUSION

Simulations of both GJL 275/190 and GJL-250 are the same in Magma5 and there are no differences between the two materials during simulations. Therefore they share the same results and are bundled together. To find when the most stress is relieved the time, stress and temperature is plotted for each run. In figure 6.4 the stress relieving process is showcased and the most stresses have been released by the time the temperature is at its peak. Meaning the majority of the stress relief has already occurred before phase 2 has started.

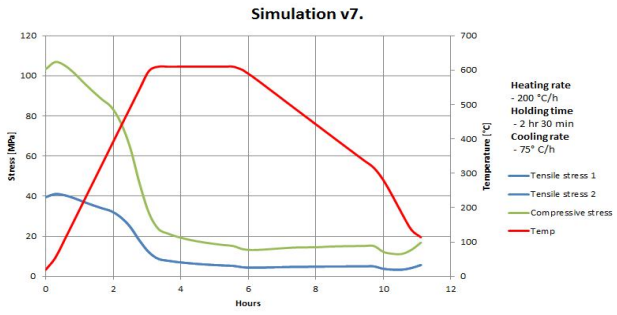

Simulation v7 of stress relieving over time. The red curve shows the temperature over time which is followed by the stress relieving effect.

Fig shows the stress relieving effect when the hold time is shortened from 2.5 h to 1h 15min. Both the tensile and compressive stresses have changed but only slightly compared to v7 in fig..

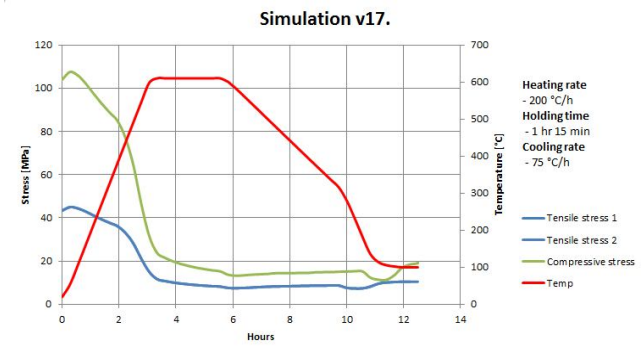

Fig. Simulation v17, from drawing with 1h 15min h hold time. Tensile stress 1 & 2 are the same.

Figure 6.6 shows the stress relieving when the cooling rate is increased from 75 °C/h to 150 °C/h. No major difference of the residual stresses can be observed by increasing the cooling rate from the simulation program. A concern regarding the later versions of the simulation is the dip in stress at the 8:30 mark. This is thought to be an accumulated error and gets progressively worse. It is possible that the change in cooling rate is the cause of the dip due to different values and more extreme parameters cause a larger change in curve.

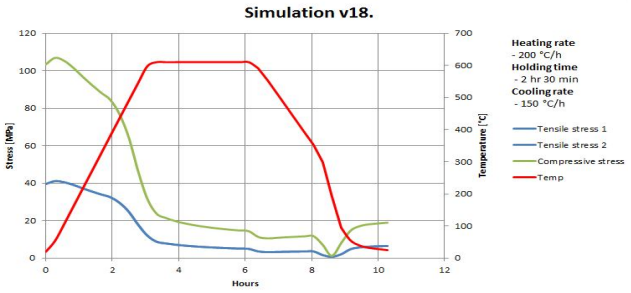

Fig. Simulation v18, drawing with a faster cooling phase of 150 °C/h.

Table 6.1 shows the remaining residual stresses after the simulated heat treatments, no major effect is obtained by either of the hold time or cooling rate separately. Combining the two parameters seems to have a synergetic effect and increases the residual stresses in both tensile and compression with an estimated 40% compared to each of the parameters alone.

Table. The simulated residual stresses after heat treatment from drawing.

Simulation:	Tensile stress point 1	Tensile stress point 2	Compressive stress point 3
From drawing (v7)	10,8	5,3	-23,1
Low hold time	12,6	4,65	-19,9
High cooling rate	12,3	4,7	-19,3
No hold time + high cooling	18,2	9,7	-33,5

VERIFICATION OF SIMULATION MODEL

By comparing the practical testing and simulations it can be seen that the simulations tend to have higher residual stresses compared to the reference lattices tested. In the figure below there is a clear difference in cooling rate between the real material and the simulated one. Another observation is that the phase transformation that occurs at ~720 °C, from austenite to pearlite, is non-existent in the simulation. When this transformation occurs in the physical material it generates heat and slows down the overall cooling rate of the material. Due to the absence of the transformation in the simulation no such reduction of the cooling rate exists. Therefore the cooling is much more rapid, creating a shift in the plot, generating a bigger discrepancy between the experimental and simulated case, especially after 730 °C. In the simulation this rapid cooling is reflected in the residual stresses, yielding values higher than the physical material.

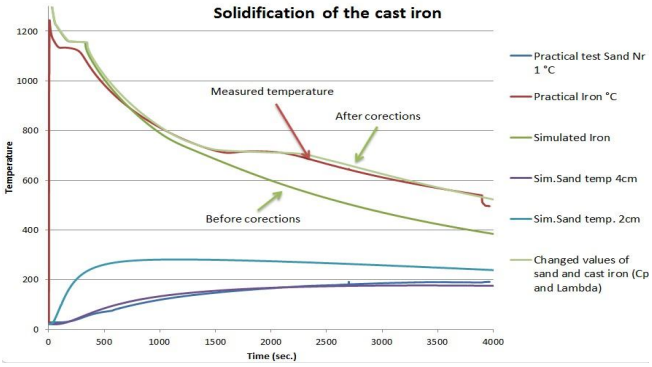

Fig. Calibration of the simulated solidification process of GJL-250.

In an attempt to make the simulation and the physical solidification process as similar as possible changes were done to material parameters in the Magma database. By changing the heat diffusion and thermal capacity of both the moulding sand and the iron the overall residual stresses were reduced in the simulation. The reduction was small and the improvements didn't make any major changes to the resulting stresses calculated by Magma5. The reduction was a total 9 MPa in compressive lowering the stress to 98 MPa.

The stresses in tensile mode did not change more than 2 MPa in the simulation with previous mentioned improvements. All of the values from the simulation before and after can be seen in Figure below.

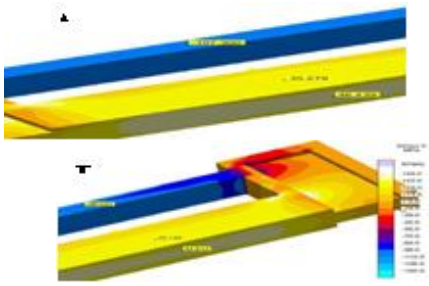

Fig. In the figure to the left (A) is the simulation before the changes to the material parameters and to the right (B) are the updated parameters with a lower stress.

RESIDUAL STRESS MEASUREMENT

This chapter shows all the resulting measurements of residual stresses. The changed parameters and resulting stress values will be compared to each other to find the most optimal heat treatment and the valuation of each change.

The residual stress is measured after solidification to get the reference stress for each material. These stresses will be used as a baseline before the heat treatments. The below figure shows how the measured stress between the materials. It's clear that the residual stress after solidification varies to the materials strength.

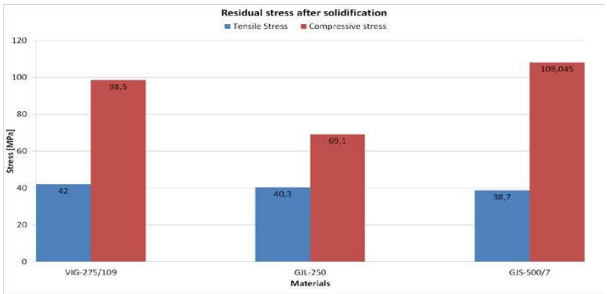

Fig. The reference residual stress as cast for each investigated material

3D SCANNING THE COMPONENT

To investigate a possible bending load case in the stress lattice the geometry was scanned before and after sectioning to see how the deformation took place. The scanning was performed on stress lattice R3 and R4 (Reference 3 and Reference 4, two as-cast lattices) and resulting strain is shown in figure. The significant deformation is along the X-axis, as desired. In R4 this is the case, less than 10% has been deformed along the Z-axis (Bending direction) and is therefore not presented in figure below . However, in R3 this is not the case; any deformation along the X-axis is less than that of R4's values and there is an equal amount of deformation along the Z-axis in the other half of the lattice. Analyzing both of these cases raise the question if some other lattices have deformed the same way as R3.

Regarding the bending and the presumed effect it might have on the overall stress results some calculations have been made, assuming an exaggerated dislocation along the Z-axis of 0.1mm, ten times the value seen in R3. With this exaggeration a difference of 40% could be created between the top and bottom side of the lattice. From this the conclusion is that these results show that the bending seen in the lattices is not causing the large irregularities of stress values measured. Using strain gauges on both sides and taking the average of the two values eliminates this error as well.

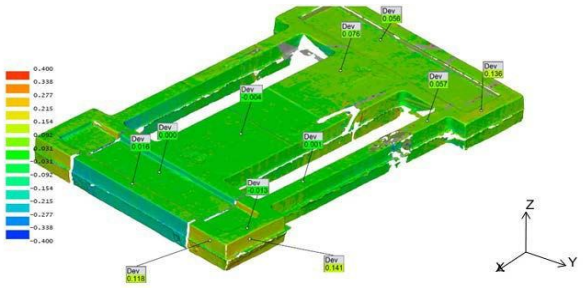

Fig. Shows the scanning of lattice R3. Deviation after sectioning is measured in mm. The marked points on the surface indicate the deformation. The deviation is significantly larger in x-direction, but the bending case in y-direction can't be ignored.

CAST IRON VIG 275/190

Find the resulting temperature vs. time plots of each HT trial see appendix (Heat treatments). All parameters for heat treated lattices are introduced in the method chapter. Following will describe the result and variation between the heat treatment runs. Resulting stresses are presented from the experiments in this chapter, both from the sectioning and the result of the different heat treatments performed. The stress results are presented in table.

Table. The resulting stress values are calculated to compensate for the bending load case in both compressive and tensile sections. *Values from HT-SL did not correspond with the stress case and are therefore omitted.

Lattice	Average Compressive MPa	Average Tensile MPa
R1 (No heat treatment)	110	37
R2 (No heat treatment)	90	53
R3 (No heat treatment)	93	37
R4 (No heat treatment)	101	41
Average Reference stress	98,5	42
HT-SL (Skövde heat treatment large oven)	Removed*	Removed*
HT-SS (Skövde heat treatment small oven)	12	14
HT-1 (heating 67 °C/h)	27	9,6
HT-2 (heating 200°C/h)	33,3	3,6
HT-3 (no hold phase)	34	13
HT-4 (5h hold phase)	24	9,3
HT-5 (150 °C/h cooling rate)	29,2	11,9
HT-6 (400 °C drop temperature)	10,9	30,8
HT-7 (no hold time and 150 °C/h cooling rate)	49,7	17,1
HT-8 (redo the HT-2)	31,3	10,9
HT-9 (time efficient HT of Skövde)	31,3	10,9
HT-10 (The HT- of Skövde)	17,6	6,4

The Fig shows the remaining residual stress after heat treatment. As shown varying heating rate between 67-200 °C/h has a significant effect on the remaining stress. The hold time at 610 °C also have a significant effect on the residual stress. Cooling rate and drop temperature, however, not showing any larger effect on the stress results. By combining high heating- and cooling rates and no hold time the stresses are much higher which is proven with the last treatment (HT-7).

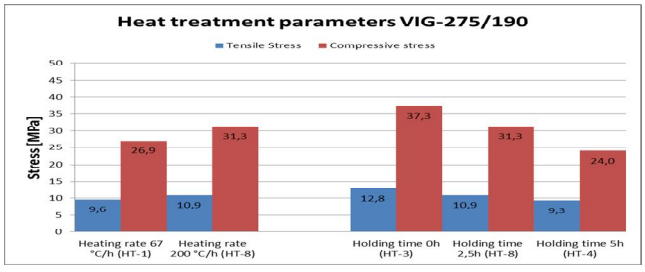

Fig. Heat treatment parameters effect on residual stresses

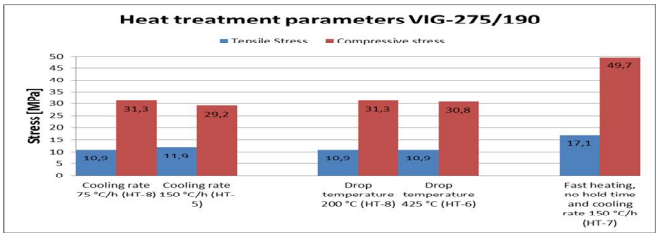

Fig. The effect of changing cooling rate and drop temperature on VIG-275/190

At last the current used heat treatment cycle in Skövde is compared to what is evaluated as a time saving heat treatment cycle based on result from previous changed parameters (trial 9). As shown, the heat treatment used today at Skövde foundry obtains much lower residual stress. This is mostly an effect of combination of parameters. The previous heat treatments only change one parameter each run and will therefore not obtain as high relieving effect as Skövde HT.

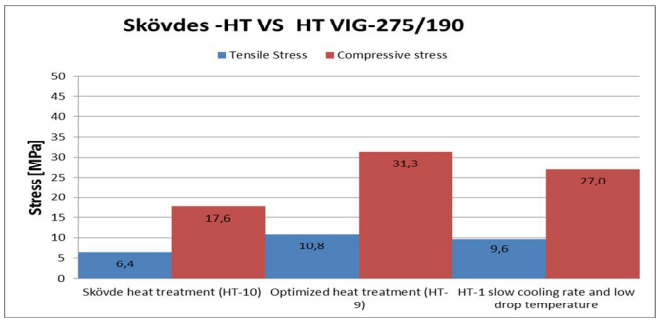

Fig. Stresses measured from the suggested rapid HT and the current HT in Skövde foundry.

The previous table shows the effect of hold time which highlights the importance for the material to spend time at high temperature. From the HT plots (Appendix B) the time spent above 500 °C is calculated and plotted against the stress relief. The plot only considers the time spent over 500 °C regardless of rapid heating, cooling rate and drop temperature since this indicates to be the most important factor of stress relieving. From the plot a second order relationship exists between relived stress and time spent above 500 °C. The assumption is that the curve will flatten out close to 10 hours, shown in Figure.

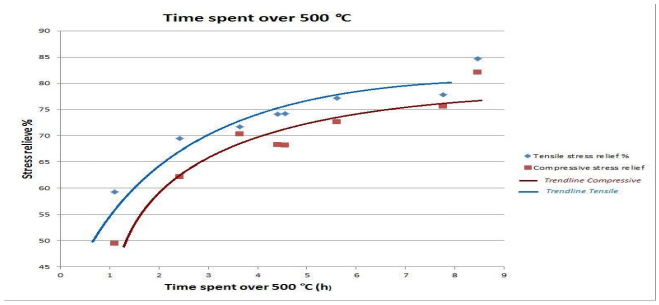

Fig. Stress relieve in % compared to the time spent over 500 °C

CAST IRON GJL-250

The unalloyed cast iron, GJL-250 responded well to the heat treatment and all tested parameters had an effect on

the resulting residual stresses. Holding time was still the most influential parameter in the VIG 275/190. The trend of the holding time is seen clearly in table Figure 6.23. Increased cooling rate and drop temperature seemed to increase the residual stress level, something not observed in VIG 275/190. Having no hold time with cooling rate and drop temperature according to the test plan provides a significant reduction in residual stresses compared to the reference. With only 75 minutes holding time the residual stresses are halved relative to the heat treatment with no holding time. Compared to the reference lattice with no heat treatment the stresses had been reduced with ~75%. Due to having only 9 lattices to use for the experiments no synergy effects were investigated and all tests have only had one varying parameter.

HT-8 was the last heat treatment performed and was done to investigate the buildup of residual stresses and to provide insight in the casting process. The temperature of the lattice, at 610 °C is close to the same temperature as the cast iron has when the mould is broken up and separated from the goods.

Heating rate was not investigated in GJL-250 due to limited amount of stresslattices. Furthermore, investigating heating rate was only done to VIG-275/190 in order to provide information regarding Skövde Foundry's own heat treatment.

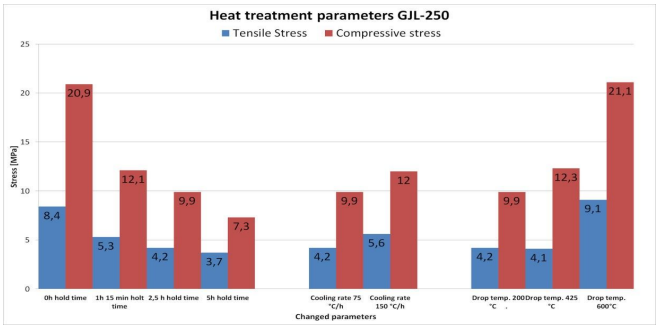

Fig. The residual stress after HT of GJL-250.

When all HT are performed they are summarized in Figure 7.24 the trend shown by VIG 275/190 is not as clear for GJL-250. Residual stresses are more easily removed in the un-alloyed material and parameters such as cooling rate and drop temperature also seems to have affected the resulting stresses. The scatter is more apparent but still a trend shows that the time over 500 °C is important.

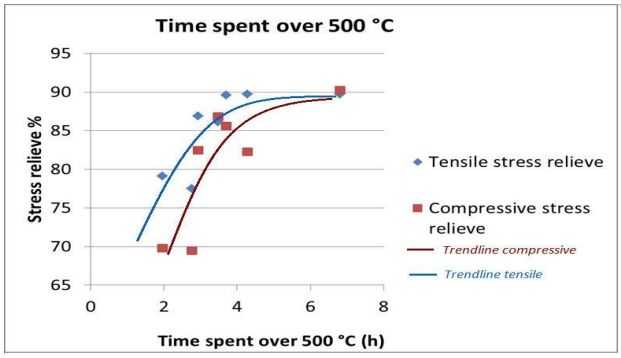

Fig. The stress relieve vs. time spent over 500 °C, GJL-250. Cast iron GJS-500-7

With four lattices available for heat treatment some adjustments were made in order to fully focus on the most important parameters. HT-2 is the heat treatment described in the plan and will provide a reference value that can be compared with the grey irons. The other heat treatments (HT-4, HT-5, and HT-6) had the same profiles as for the grey irons. Seen in Figure, is the stress after each HT. HT-4 seemed to respond well to the increased hold time and showed low stress. Comparing HT-2 with HT-5 and HT-6 shows no remarkable difference of changed parameters in the cooling phase. The differences are roughly within 2 MPa in compressive stress and less than 2 MPa in tensile stress. The increased stress by higher cooling rate indicates to some effect of increasing the cooling rate above 400 °C. In short it looks like the GJS-500-7 has a tendency for faster creeping and responds quickly to the HT.

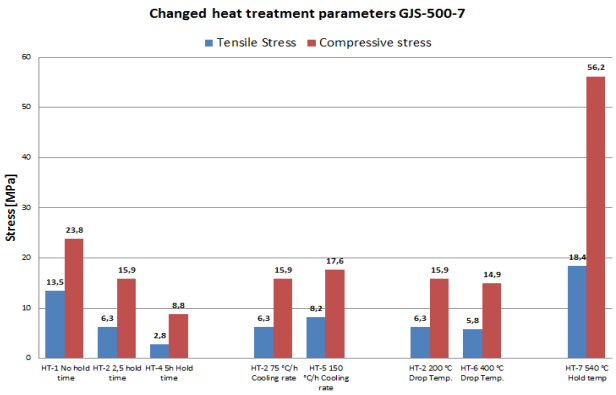

Table. The residual stress after heat treatments conducted on GJS-500-7

Comparing the results with simulations shows once more that Magma5's model of GJS-500-7 is not fully correct. The values provided from the simulations were far above the actual stress with values more than twice the amount of stress. The stress values from the simulations have been presented in table. Still the simulations predicted the effect of the different parameters correctly and HT-2, HT-5, and HT-6 had similar

values in the simulation, just as the measured values seen in the table above. Yet again do the tests confirm the importance of holding time and the residual stresses are reduced significantly with a longer holding time. From HT-7 where the holding temperature was reduced from 610 °C to 540 °C confirms that that reducing the holding temperature can severely affect the residual stresses. Comparing HT-1 and HT-7 shows the difference between having a higher temperature or longer holding time.

COMPARISON OF THE MATERIALS

In Figure all investigated cast iron alloys are presented with the stresses as cast and after HT-2, which is the recommended heat treatment from Volvo. From the table there is a clear difference seen between the alloys not using Mo and Cr. Both the unalloyed cast iron, GJL- 250 and the ductile iron GJS-500-7 have roughly 14% of the stress before HT, while in VIG 275/190 the difference is 33/25% in compressive and tensile respectively. The difference seen in relaxation between tensile and compressive in all the alloys is due to the variation in cross section area and volume. This is especially noticeable in the case of VIG 275/190. Another value to note is a low compressive stress in the GJL-250 reference and this low value is assumed to be due to an errant strain gauge, without that value the stress is 76 MPa. This assumption is because the simulation has shown reliable values regarding the GJL-250 cast iron.

Furthermore, the HT-2 has proven to be successful for the two cast irons not containing Mo or Cr and most of the residual stresses has been relived during the process. With regards to VIG- 275/190 a 2 hour and 30 min hold time is not enough to fully reduce the stress.

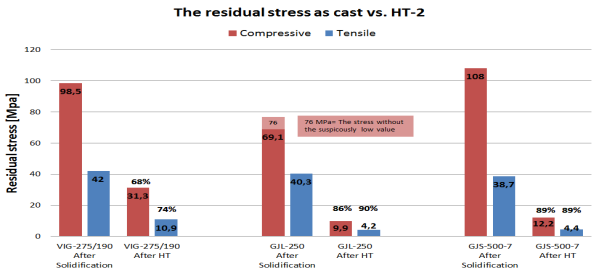

Fig. A comparison of residual before and after HT-2. The % values show the residual stress reduction during HT.

In Figure the simulations of casting process and heat treatment (drawings) are compared to the practical testing. For the VIG-275/190 simulations predict higher stress after solidification and lower stress after heat treatment, i.e. a higher relieving effect. In the ductile iron GJS-500-7 the simulations also predict a higher stress after solidification but also higher stress after heat treatment.

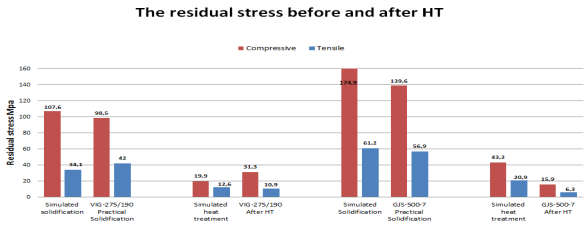

Fig. Comparison of simulations and experimental test on residual stresses. GJL-250 is not included since it uses the same simulation data as VIG-275/190.

EXPERIMENTAL VERIFICATION OF MATERIALS

The verification of the three materials analyzed is done in order to confirm the composition of the material, the microstructure, hardness and the distribution of the ferritic and pearlitic matrixes. Stresses presented previously are valid for the type of materials presented in this chapter.

GREY IRON, VIG-275/190

The hardness test shows that the hardness differs between the tensile and compressive sections. The assumption is that the cooling in these sections is different, with a higher cooling rate in the compressive section increasing the hardness. The increased cooling rate changes the microstructure towards smaller graphite and finer pearlite that will provide a higher hardness. The conclusions of hardness tests are the values are within expectations and exceed the specified minimum requirement, table. In the compressive section of the GJL- 250 the hardness differentiates a lot from the tensile section. Regarding the ductile iron, GJS- 500-7 the hardness value is high and some values are above the specification. The same hardness values were seen in both SKF and Skövdes lattices and hardness values this high indicates incorrect distribution of pearlite and ferrite, caused by larger undercooling.

Table, Hardness measurement (Brinell 2,5mm with 187,5kg). Each value is a mean value of three indentations.

Hardness	VIG-275/190	Grey iron, GJL-250	GJS-500-7 SKF (R2)	GJS-500-7 Skövde (R1)
Compressive	258	228	240	247
Tensile section	231	185	231	218
STD	min 190	190-240	170-230	170-230

The amount of graphite in VIG-275/190 is varying between the tensile and compressive section. The tensile section obtains a graphite amount of 11,4% and the compressive is 8,8% the differences in amount of graphite is influenced by the polishing of the micro samples. Graphites loosely fixated and are very easily removed during the grinding process, thus potentially creating this error. The tests were performed on the reference lattice, R1. No visible difference can be seen between the two samples; the graphite structure looks similar for both images and has a formation of the graphite is I accordance to *EN ISO 945-1:2008*. The type of flakes is the most similar to A + E structure.

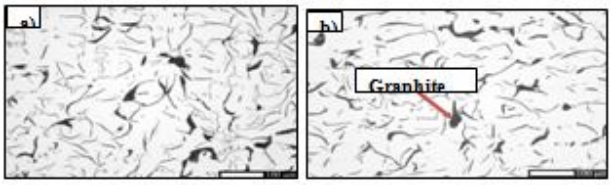

Fig. The microstructure of graphite VIG-275/190. a) The compressive section b) The tensile section.

When the samples have been etched the lamellar structure of perlite becomes visible, easier to see around the lighter sections. This pearlite structure is also obtained in darker sections; it depends on from which angle the sample is cut. Along the graphite edges there can be small amounts of ferrite, often seen as white sections along the graphite flakes. There is also a slight discoloration in the tensile section, seen as yellow-blue color. Lastly there is a small scatter of grey circular sections (easiest seen in the lower left corner in the compressive section). This is presumed to be Manganese-sulfides (MnS). These particles provide a lubricating effect during cutting and are desirable in small quantities.

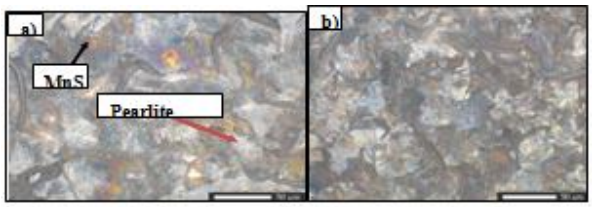

Fig. a) Tensile section b) Compressive section. The microstructure of VIG-275/190 etched with 1% Nital acid.

Tensile test is performed to confirm that strength is according to specification. As shown in Figure the lattice is cut in 6 tensile samples and sent to be manufactured as tensile specimens. Three specimens from the compressive section and three from the tensile section are cut out. The test bars are of type 7C35.

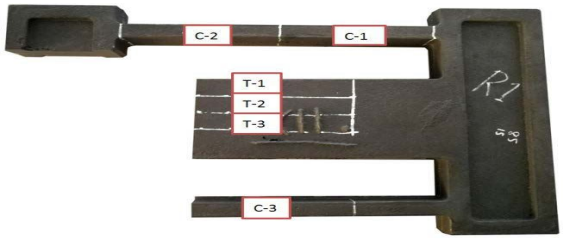

Figure. The location of where the tensile test specimens are cut out.

All components were not fully functioning in the testing machine when the tensile testing started and therefore C-1 and C-2 are not properly set up (missing values from extensometer). C-3 had its fracture outside of the extensometer gauge and broke very close to its attachment but the result seems to fall within the expected value.

All six tested bars fulfill the requirements of at least 275 MPa (Rm). The compressive bars show a higher tensile strength and this is due to the higher cooling rates in those sections of the lattice. The microstructure is finer and therefore the strength is higher given by the Hall-Petch relation. T-2 had low values compared to the other tensile bars and a graphite pore is in the crack zone which would explain the low value, shown in Figure. The testing was conducted by the standard EN ISO 6892-1 A222.

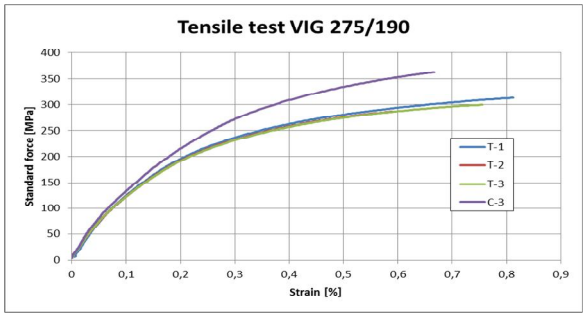

Fig. Tensile tests C-1 and C-2 were ignored due to invalid values and T-2 is behind T-1 and T-3.

GREY IRON, GJL-250

In the microstructure samples from GJL-250 the compressive section shows a less distributed graphite structure, 6.20. The graphite in figure (a) is all type-A shaped, the wanted shape in grey cast iron, Figure 6.20 (a) in the thicker section of the lattice. In the thinner part section the graphite shape is changed to B-type graphite due to the undercooling experienced in the section. There is also the transition shape graphite type-D present as well with some smaller portion of type A graphite. It has been stated previously that the hardness of the compressive section is 40 HB higher than the tensile section which would indicate that

the microstructure is different and material properties might vary between the thinner and thicker sections.

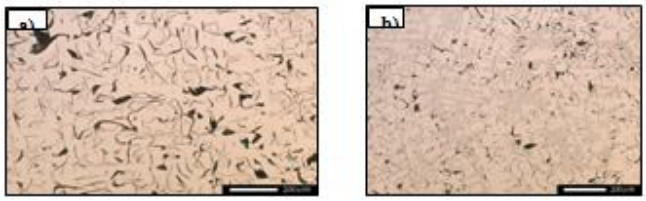

Fig. a) Tensile section microstructure (thick section), b) microstructure of compressive section (thin section)

Figure shows the microstructure after etched with Nital acid 3%. Etching is done to reveal the pearlite structure of the cast iron and it can be clearly seen in both Figures below. Looking at the tensile section (a), there is a lot of ferrite present which is a "defect" due to slow cooling. Requirements for grey cast irons are less than 1% ferrite matrix but the amount of ferrite detected here is above the recommendations.

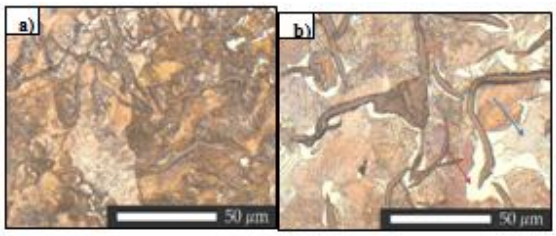

Fig. a) Tensile section. b) Compressive section. Etched micro-samples shows the microstructure of the perlite and ferrite around the graphite is clear in sample b. Blue arrow shows a typical perlite structure and red arrow shows the ferrite (sample b).

A brief overview of GJL-250 is given from the two tensile bars tested. Both tensile bars are within the specifications with T-1 being on the verge of 250 MPa tensile strength.

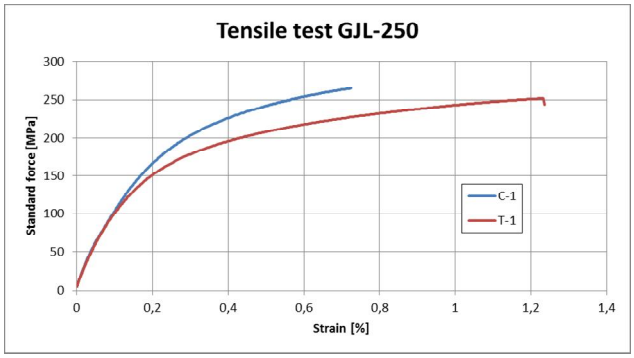

Fig. Tensile test of GJL-250. Red curve is the tensile and blue is the compressive section.

DUCTILE IRON GJS-500-7

Micro-samples are manufactured to investigate the nodule structure and measure the nodularity and nodule count, shown in Figure 6.34. There are clear differences in nodule sizes and this is due to the cooling rate being higher in the thinner, compressive section.

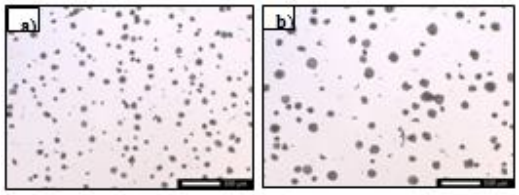

Fig. a) Compressive section, Skövdes lattice, nodularity 90% b) Tensile section, nodularity 86%.

Etching with 3% Nital acid will show the perlite structure. Shown in Figure the bright sections around the graphite is ferrite. The ratio of ferrite/pearlite should be around 50/50 but by analysis the ratio is 30/70. This would also explain the hardness values being on the verge of too high.

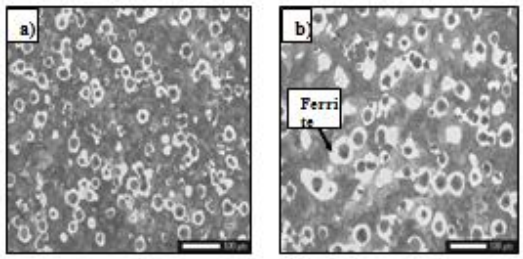

Fig. a) Compressive section of Skövdes lattice, small graphite due to a rapid solidification b) Tensile section, obtains larger graphite nodules and high amount of surrounding ferrite. High amount of perlite is found in both sections.

The tensile tests of GJS-500-7 show that both bars are outside of the specifications. This is explained by the high amount of pearlite seen in the microstructure. Both the elongation and tensile strength, seen in Figure is more similar to GJS-600-5.

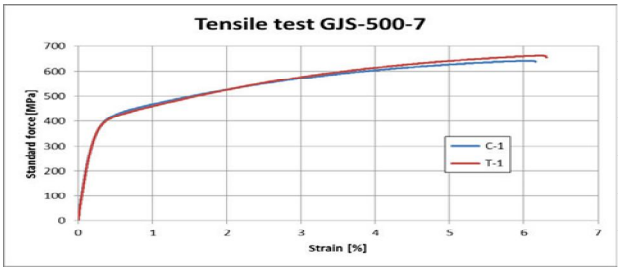

Fig. Tensile test of GJS-500-7. Both curves are not within the specifications.

V. CONCLUSION

Conclusions are the summary of the most important findings

SIMULATION BY MAGMA 5

- The simulations in all cases show higher residual stresses after solidification compared to the measurement. This can partly be explained by the missing phase transformation at 723 °C from austenite to pearlite. By modification of the specific heat capacity of sand mould and cast iron material the cooling rate can be corrected to match the measured temperature. By making this change the result of the simulation are more in line with the practical measurements.
- In simulation of the HT, stress relieving is observed to be finalized reaching the peak temperature at 600 °C, after this point the stress relieve is no longer significant. The relieving trend is not like what is stated in the theory of stress relieving depending on creep or from what's shown by the practical testing.
- The effects of changed cooling rate and drop temperature are difficult for the software to predict. The simulations do not show any significant effect of a rapid cooling.
- The simulations consecutively show lower stress in comparison to the practical case after the heat treatment (GJL-300 compared to VIG-275/190).

Simulations of GJS-500-7 are not following the same trends as grey iron. The stress after both solidification and heat treatments shows higher values compared to the measurements. The relieved stress after heat treatment is 89% (both tensile and compressive). The simulation predicted a relieving of75%/63% (Compressive/Tensile) for the ductile iron which is significantly higher. This indicate that Magma5 has difficulties predicting the effectiveness of the HT and estimates a higher value than the actual case. *Grey iron, VIG-275/190*- Mo is a potent alloying material which increases both the tensile strength and mechanical properties at elevated temperature. This results in higher residual stress as well as making the heat treatment less effective. (Cr is also increases the tensile strength but not to the same degree as Mo.) Cr also lowers the graphite content in the material and might cause additional shrinkage in the casting process. The time spent above 500 °C shows a clear trend which is important to point out for future work and recommendations.

Grey iron, *GJL-250* - Comparing the un-alloyed grey iron to VIG-275/190 most results fell within the predictions. The un-alloyed grey iron is responding more easily to the heat treatments, due to a lower tensile strength and no alloying elements that counteract the creep. This is also stated and explained in detail in the theoretical background. The micro-samples of the GJL-250 showed significant variances in hardness and microstructure. Hardness of 40 HB is due to effect of undercooling the material is shown in the thin section. From the tensile test, large differences were seen between the compressive and tensile bars and neither of them are within specifications. However, the chemical analysis showed that the material was within the specifications. Therefore, the assumption is that the stress values measured from the lattices are still valid and the results are valid.

GJS-500-7- The ductile iron obtains more residual stress after solidification compared to the grey iron materials, which is related to its higher tensile strength. The heat treatment test confirms that the ductile iron easily relieves residual stress compared to VIG-275/190, most probably due to less alloying elements and no Mo or Cr. The cooling rate seems to have some effect on the residual stress but not to the same degree as hold time. Creep does not occur below 425 °C and was shown by varying the drop temperature. The hold time is the most important parameter, like the grey irons. The hardness of the GJS-500-7 was at the upper limit due to the amount of pearlite being too high. The chemical analysis shows no values outside the specifications. The higher grade ductile iron GJS-600-5 has more in common with the material analyzed and has the same pearlite/ferrite ratio. Even if the material is more similar with GJS-600-5 the results are still valid and the results found can be applied to both materials.

Regarding the stress relieving of HT-2, VIG reduces the stress with about 70%, GJL with 86/90% and GJS with 89/89% (compressive/tensile). This confirms the effect of alloying elements in the VIG-material and shows that GJS-material has easier to reduce residual stress compared to the alloying grey iron.

PRACTICAL TESTING

Comparing the obtained residual stress of the lattices, the following results can be stated for each material:

Grey iron, VIG-275/190:

- In VIG-275/190 the time spent over 500 °C is the most important factor to relieve residual stresses. Alloying elements Mo and Cr lowers the creep and diffusion in the material, especially in the 0-400 °C range and makes the material less responsive to heat treatments. This is stated with HT-7, when the drop temperature was set to 425 °C but the residual

stresses remained the same as drop temperature of 200 °C.

- Heating rate and hold time are parameters with most effect on the stress relieving process.
- A low cooling rate from temperatures below 425 °C are not significantly important, due to the creep resistance at lower temperatures.
- Mo and Cr forms a finer cell structure and should by theory increase the potential of stress relieving. But this effect is fully counter-acted by Mo which decrease the effectiveness of creep.

Grey iron, GJL-250:

- Responds easy to the HT and obtains higher amount of residual stresses relived compared to VIG-275/190. This is explained by the fact that the material has easier to creep and diffuse.
- Stress relieved mostly by a longer hold time, but also cooling rate and drop temperatures are shown to be of significant importance, due to higher creep at lower temperatures.
- From experimental trials it has been shown that a rapid cooling from 600 °C generates less relieving compared to drop temperature of 200 °C, this observation can be used considering the sand mould opening temperature.

Ductile iron EN-GJS-500-7:

- Obtains highest amount of residual stresses as cast compared to the grey iron materials, due to its high strength. This trend is mostly shown by simulations, when measuring the practical lattices the stress after solidification did not have variation as simulations predicted.
- The HT confirms that ductile iron has easy to relieve residual stress compared to grey iron, most probably due to less alloying elements.
- The cooling rate shows to have some effect on residual stresses.
- Increasing drop temperature to 425 °C will not have an effect on residual stresses.

VI. FUTURE WORK

The practical testing had a limited amount of stress lattices. With a higher amount of test lattices a wider range of parameters and their combinations can be examined. Also, an optimized complete heat treatment cycle could be formed for each specific material.

Further investigation of how high temperatures you can reach (hold temperature) without affecting the microstructure and mechanical properties would be interesting to investigate. To reach as high temperature as possible would make creep higher and accelerate the stress relieving. In the pre-study three hold temperatures have been investigated and their respective hardness have been compared. The results indicate that a hold temperature of 650 ° C is too high and changes the mechanical properties of the material,

For the material GJS-500-7 it would be interesting to further investigate how low hold temperature you can reach with same relieving effect to save both energy and time.

REFERENCES

[1] G. I. Sil'man, V. V. (2003). Effect of Copper on Structure Formation in Cast Iron. In *Metal Science and Heat Treatment* (pp. 254-258).

[2] G. Totten, M. H. (2002). *Handbook of Residual Stress and Deformation of Steel.* ASM International.

[3] Gjuterihandboken.se. (2015, 01 01). *http://www.gjuterihandboken.se/handboken/3-gjutna-material/32-graajaern*. Retrieved from Gjuterihandboken: http://www.gjuterihandboken.se/

[4] Gundlach, R. B. (2005). The effects of alloying elements in the elevated temperature properties of Grey irons. Michigan: AMAX material research center.

[5] Janowak, J. F., & Gundlach, R. B. (2006). *A Modern Approach to Alloying Gray Iron.*American Foundry Society.

[6] Johannesson, B., & Hamberg, K. (1989, 11 24). *Spännings/töjnings-egenskaper hos gråjärn avsett för cylinderhuvuden [Internal report LM-54159]*. AB Volvo. Technological Development.

[7] Holtzer, M. G. (2015). *Microstructure and Properties of Ductile Iron and Compacted Graphite Iron Castings.* Springer.

[8] Magmasoft. (2017, 01 23). *www.magmasoft.com*. Retrieved from http://www.magmasoft.com/en/solutions/ironcasting.html : http://www.magmasoft.com/en/solutions/ironcasting.html

[9] Pentronic. (2017, 04 11). *http://www.pentronic.se/*. Retrieved from http://www.pentronic.se/start/temperaturgivare/teori-om-givare/tabeller-och- polynom.aspx.

[10] Schmidt, P. (2016). *Cast Iron*. Volvo Materials Technology.
Sn-castiron.nl. (2009). Retrieved from http://www.sn-castiron.nl/en/castiron/en_gjl.html: http://www.sn-castiron.nl/en/castiron/en_gjl.html

[11] Shaw, M.C. "Principles of Material Removal," Mechanical Behavior of Materials, Vol. 1, 1979, p. 227-253.
[12] Ernst, H. and M. Merchant. "Chip Formation, Friction, and High-Quality Machined Surface, " ASM Symposium on Surface Treatment of Metals, 1941, p. 299-335.
[13] Degarmo, E., Black, J., and Kohser, R. Materials and Processes in Manufacturing, Wiley and Sons Inc. 2003.
[14] Taylor, F. W. "On the Art of Cutting Metals," ASME Transactions, Vol. 28, 1906, p. 31.
[15] Zimmerman, C., Boppana, S., and K. Katbi. "Machining of Specific Metals and Alloys: Machinability Test Methods," ASM Handbooks – Online, Vol. 16. 2009.
[16] Bhadeshia H K D H and Edmonds D V. Analysis of mechanical properties and microstructure of high silicon dual phase steel. Metal Science, 1980, 14(2): 41–49.
[17] Voigt R C, Bendaly R, Janowak J F, et al. Development of austempered high silicon cast steel, AFS Transactions, 1985, 93: 453–462.
[18] Park Y J, Gundlach R B, Janowak J F. Monitoring the bainite reaction during austempering of ductile Iron and high silicon cast steel by resistively measurement. AFS Transactions. 1987, 95: 411–416.